

MFTune: An Efficient Multi-fidelity Framework for Spark SQL Configuration Tuning

Beicheng Xu^{†*}, Lingching Tung^{†*}, Yuchen Wang[†], Yupeng Lu[†], Bin Cui[†]

[†]School of Computer Science, Peking University, China

[†]{beichengxu, lingchingtung, wychen}@stu.pku.edu.cn, [†]{xinkelyp, bin.cui}@pku.edu.cn, [†]

ABSTRACT

Apache Spark SQL is a cornerstone of modern big data analytics. However, optimizing Spark SQL performance is challenging due to its vast configuration space and the prohibitive cost of evaluating massive workloads. Existing tuning methods predominantly rely on full-fidelity evaluations, which are extremely time-consuming, often leading to suboptimal performance within practical budgets. While multi-fidelity optimization offers a potential solution, directly applying standard techniques—such as data volume reduction or early stopping—proves ineffective for Spark SQL as they fail to preserve performance correlations or represent true system bottlenecks. To address these challenges, we propose MFTune, an efficient multi-fidelity framework that introduces a query-based fidelity partitioning strategy, utilizing representative SQL subsets to provide accurate, low-cost proxies. To navigate the huge search space, MFTune incorporates a density-based optimization mechanism for automated knob and range compression, alongside an adapted transfer learning approach and a two-phase warm start to further accelerate the tuning process. Experimental results on TPC-H and TPC-DS benchmarks demonstrate that MFTune significantly outperforms five state-of-the-art tuning methods, identifying superior configurations within practical time constraints.

PVLDB Reference Format:

Beicheng Xu^{†*}, Lingching Tung^{†*}, Yuchen Wang[†], Yupeng Lu[†], Bin Cui[†]. MFTune: An Efficient Multi-fidelity Framework for Spark SQL Configuration Tuning. PVLDB, 14(1): XXX-XXX, 2020. doi:XX.XX/XXX.XX

PVLDB Artifact Availability:

The source code, data, and/or other artifacts have been made available at <https://github.com/Elubrazione/MFTune>.

1 INTRODUCTION

The recent explosion of data has catalyzed the widespread deployment of large-scale query systems, such as Hive [47], Presto [41], and Spark SQL [2]. Among these, Spark SQL has emerged as a premier choice for industry-scale data processing due to its robust integration with the Spark ecosystem [60] and its superior performance in handling complex analytical workloads. It serves as a

This work is licensed under the Creative Commons BY-NC-ND 4.0 International License. Visit <https://creativecommons.org/licenses/by-nc-nd/4.0/> to view a copy of this license. For any use beyond those covered by this license, obtain permission by emailing info@vldb.org. Copyright is held by the owner/author(s). Publication rights licensed to the VLDB Endowment. Proceedings of the VLDB Endowment, Vol. 14, No. 1 ISSN 2150-8097. doi:XX.XX/XXX.XX

* Beicheng Xu and Lingching Tung contribute equally to this paper.

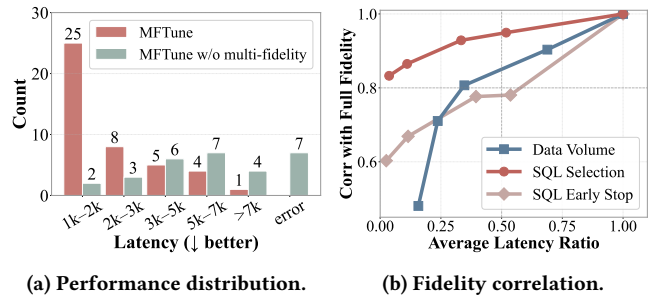


Figure 1: Analysis of multi-fidelity mechanism on TPC-DS (600GB). (a) Performance distribution of configurations evaluated within a 48-hour budget, comparing MFTune against a single-fidelity variant. (b) Fidelity correlation. We evaluate the representativeness of three proxy methods by randomly sampling 50 configurations from the search space. The proxies include: 1) Data Volume: scaling the dataset across {30,100,200,400,600} GB; 2) SQL Early Stop: executing the first {1/27,1/9,1/3,2/3,1} of the total SQLs; and 3) SQL Selection: selecting representative SQL subsets at fidelity levels 1/27 to 1 based on Section 6.1. Each point represents the Kendall's Tau correlation between proxy and full-fidelity performance, plotted against the average latency ratio (proxy latency relative to full-fidelity latency) across 50 configurations.

foundational component for critical downstream applications like database management [57]. However, the efficiency of Spark SQL is heavily dependent on more than 200 configuration knobs that govern system behaviors like memory management and shuffle partitioning [45]. For example, the knob *spark.executor.memory* specifies the amount of memory for an executor process. An excessively large value increases garbage collection time, whereas an excessively small value may cause out-of-memory errors. Because the default settings are often suboptimal for specific workloads and the search space is prohibitively large, manual tuning by database administrators is both time-consuming and far from optimal.

To find optimal configurations for Spark SQL workloads, various automatic configuration tuning methods have been proposed [5, 8, 26, 29, 42, 56]. These methods typically adopt the Bayesian Optimization (BO) framework [12, 44] to sample promising configurations, which iteratively samples configurations and replay the workload to model the relationship between system performance and parameters. However, these methods suffer from several fundamental challenges when applied to Spark SQL:

C1. Prohibitive evaluation costs. Spark SQL workloads typically handle massive data volumes and consist of multiple queries,

leading to execution times that span hours or even days. However, existing tuning methods often rely on full-fidelity evaluations (executing the entire original workload) [8, 26, 29], which limits the number of configurations that can be explored within a finite tuning budget. A potential solution to mitigate this bottleneck is to adopt Multi-Fidelity Optimization (MFO) [7, 27, 31]. MFO leverages low-fidelity evaluations, which are faster but approximate the full-fidelity results, to efficiently filter out poor configurations and guide the search toward optimal regions. Our preliminary analysis in Figure 1a demonstrates the impact of this mechanism: within a 48-hour budget, MFTune successfully evaluated 43 configurations with MFO. In sharp contrast, a single-fidelity variant (MFTune w/o multi-fidelity) evaluated only 29 configurations in the same time frame, with the majority falling into higher latency buckets or even resulting in execution errors. These illustrate that relying solely on full-fidelity evaluations makes it nearly impossible to explore the vast search space effectively within practical time constraints.

C2. Inapplicability of directly applying existing MFO methods. The core challenge of MFO lies in ensuring that the low-fidelity proxies preserve the relative ranking of configurations observed under full fidelity. However, existing standard fidelity-partitioning techniques used in Automated Machine Learning (AutoML), such as training on a subset of data [20, 30, 31] or for fewer epochs [7, 16, 30], do not transfer effectively to Spark SQL. As illustrated in Figure 1b, existing proxies such as **Data Volume** and **Early Stop** fail to maintain a reliable correlation with full-fidelity performance in Spark SQL. Reducing data volume leads to a sharp decline in correlation because performance does not scale linearly; smaller datasets often underutilize cluster resources and fail to trigger the true bottlenecks encountered at full scale. Similarly, SQL Early Stop—executing only the initial queries of a workload—fails to capture the diverse data coverage and operation types representative of the entire workload. In contrast, our proposed SQL Selection maintains a high Kendall-tau correlation (>0.8) even at extremely low fidelity levels. These findings demonstrate that customizing fidelity partitioning for the Spark SQL domain is essential, as generic AutoML proxies cannot maintain the ranking consistency required for effective tuning.

C3. Huge search space and ineffective compression. With over 200 parameters, the search space of Spark SQL is prohibitively large for exhaustive exploration within a limited budget. Most existing works focus solely on reducing the number of knobs via sensitivity analysis or projection [8, 29, 54, 56]. Only a few methods [46, 65] have attempted to compress the value range. However, these approaches rely on simple bucketization or discrete historical boundaries, leaving them highly susceptible to outliers and unable to capture promising regions that were insufficiently explored in previous tasks. Consequently, achieving robust and fine-grained search space compression remains an open challenge.

To address these challenges, we propose MFTune, an efficient multi-fidelity framework tailored for Spark SQL configuration tuning. For **C1**, inspired by the success of multi-fidelity optimization (MFO) in AutoML, we design an MFO framework that performs iterative evaluations across varying fidelity levels, effectively pruning suboptimal configurations early to maximize budget efficiency. Furthermore, we incorporate transfer learning and warm-start mechanisms specifically tailored for the multi-fidelity paradigm to further accelerate convergence. Instead of conventional data reduction or

early stop, MFTune identifies a representative subset of SQL queries to serve as low-fidelity proxies. This approach preserves workload diversity and critical performance bottlenecks while significantly reducing evaluation costs (**C2**). For **C3**, the system incorporates a density-based compression mechanism that leverages SHAP values and Kernel Density Estimation (KDE) to automatically prune unimportant knobs and narrow value ranges to high-potential regions.

Our key contributions are summarized as follows:

- To the best of our knowledge, we are the first to introduce multi-fidelity optimization (MFO) into the domain of Spark parameter tuning, tailoring transfer learning and warm-start mechanisms to accommodate varying fidelity levels.
- We propose a query-based multi-fidelity partitioning algorithm to select representative SQL query subsets that maintain a high performance correlation with full-fidelity workloads.
- We introduce a unified framework for knob selection and range compression based on weighted density modeling, which captures high-potential regions accurately.
- Extensive evaluations across various benchmarks, hardware scenarios, and data scales demonstrate that MFTune significantly outperforms five state-of-the-art tuning methods, yielding 25.9%–43.1% and 37.8%–63.1% latency reduction on TPC-H and TPC-DS, respectively, within a 48-hour tuning budget.

2 RELATED WORK

2.1 Automatic System Configuration Tuning

DBMS tuning. Various automatic configuration tuning methods have been proposed to automatically recommend high-performance configurations for Database Management Systems (DBMS) [11, 66]. Among these methods, Bayesian Optimization (BO)-based methods and Reinforcement Learning (RL)-based methods have been the most widely used and achieve state-of-the-art performance. BO-based methods (e.g., OtterTune [50], ResTune [63], LlamaTune [18], OpAdvisor [65], TopTune [54]) iteratively sample configurations and replay the workload to model the relation between configuration and performance. In contrast, RL-based methods (e.g., CDB-Tune [61], QTune [25], Hunter [4], UDO [52]) use RL to predict the reward of a configuration, and explore new configurations to maximize the reward. However, RL-based methods can take many iterations to achieve good performance [56]. Additionally, some recent works utilize LLM to help tune DBMS [23, 46, 49]. Another line of studies focuses on the online setting, addressing the workload shift during the tuning process [43, 64].

Spark SQL Tuning. While DBMS tuning methods can in principle be adapted to Spark SQL, the significantly longer query execution times in Spark SQL make methods that require hundreds of iterations [4, 63, 65] extremely time-consuming. Therefore, Spark SQL-specific tuning methods are necessary. Recently, there have been some auto-tuning methods tailored for Spark SQL, which can be categorized into the following three classes: 1) Early work focused on cost modeling methods that rely on a deep knowledge of system performance to build performance models [6, 9, 51]. However, it is difficult for them to capture complex system behaviors. 2) To reduce reliance on domain knowledge, machine learning (ML) approaches employ ML techniques to build performance models [39, 58, 67],

which need a large number of training samples with high overhead. 3) Most auto-tuning methods are also based on Bayesian Optimization (BO) and strive to enhance tuning efficiency to address the validation overhead of Spark SQL workloads [1, 29, 56]. For example, TIE [5] accelerates the sampling phase of BO through an early termination mechanism, thereby reducing the tuning time. LOCAT [56] compresses the target workload after obtaining sufficient evaluation observations of the original workload, and performs BO in a reduced search space. To avoid tuning each workload from scratch, some methods leverage knowledge from similar historical tuning tasks [8, 26, 29, 42]. For example, Tuneful [8] employs a Multi-Task Gaussian Process (MTGP) to train and predict similar historical task data alongside current task observations. Online-Tune [29] and LOFTune [26] obtain optimal configurations from similar tasks for a warm start. Rover [42] accelerates tuning by weighting the BO acquisition function with historical tasks.

However, all the aforementioned methods share a common limitation: they rely on complete evaluations of the workload. Within a limited budget, it’s challenging to evaluate enough configurations on complex, large-scale Spark SQL workloads, leading to insufficient search space exploration and reduced optimization efficiency. LOCAT [56] is the only approach that considers compressing workloads, but it still relies on extensive original workload evaluations for compression. Additionally, it fully replaces original workloads with compressed ones, which lacks reliability. Overall, efficient Spark SQL configuration tuning remains a significant challenge.

2.2 Multi-Fidelity Optimization

Although system parameter tuning currently relies on complete evaluations, automated machine learning (AutoML) and neural architecture search (NAS) are exploring multi-fidelity optimization methods to tackle this challenge [10, 16, 20, 27, 40]. Typically, multi-fidelity optimization methods exploit the low-fidelity evaluations of the objective function f to guide the search for the optimum of f . Hyperband [27] (HB) dynamically allocates resources to a set of random configurations, and uses the successive halving algorithm [14] to stop poor-performing configurations in advance. BOHB [7] improves HB by replacing random sampling with BO. MFES-HB [31] combines HB with multi-fidelity surrogate-based BO. ASHA [28], A-BOHB [22], and Hyper-Tune [30] proposed to extend HB to the asynchronous case when using multiple workers, which led to significant improvement. An orthogonal line of work models the learning curves of machine learning algorithms directly [34]. These studies often use neural networks to rank learning curves across different configurations and different tasks [21, 55].

However, as analyzed in Challenge C2 (Section 1), directly applying AutoML-based MFO to Spark SQL is unreliable because standard proxies, such as data subsetting or early stopping, fail to maintain a strong ranking correlation with full-fidelity performance. These underscore the essential need for a domain-specific fidelity partitioning approach to ensure accurate and efficient tuning.

3 PRELIMINARIES

3.1 Spark SQL Background

Apache Spark [59, 60] is an open-source distributed computing system for large-scale data processing and analytics. Spark SQL is

a Spark module for structured data processing [2]. In real-world scenarios, Spark SQL workloads typically have two characteristics: 1) They often include multiple queries, as real-world productions often structure data processing tasks as multi-stage workflows. Examples include Extract, Load, and Transform pipelines in data warehousing [19] and feature generation for machine learning [13]. Similarly, commonly used benchmarks also consist of multiple queries, as shown in Section 7.1. 2) They typically process large volumes of data, spanning hundreds of gigabytes to several terabytes or more [53]. The combination of multiple queries and massive datasets makes Spark SQL workloads highly resource-intensive, often requiring hours or even days to complete. Suboptimal hyperparameter settings can further exacerbate this issue, potentially leading to execution failures. Therefore, effective performance optimization is critical to reduce both latency and costs.

The execution of Spark SQL queries is controlled by more than 200 parameters [45], which determine many aspects, including dynamic allocation, scheduling, shuffle behavior, data serialization, memory management, etc. Overall, parameter tuning for Spark SQL is essential and presents the following challenges: 1) The vast search space is difficult to fully explore within a limited tuning budget, necessitating the optimization and compression of the search space. 2) Evaluating configurations is computationally expensive, especially when suboptimal configurations drain the tuning budget without yielding significant gains. Therefore, it is crucial to avoid allocating excessive budget to evaluating poor configurations.

3.2 Problem Definition

Formally, given a target workload W , which consists of a set of SQL queries on a certain database, the goal of Spark SQL configuration tuning is to find the optimal Spark configuration \mathbf{x}^* that minimizes a pre-defined objective function. The problem definition is as follows,

$$\mathbf{x}^* = \arg \min_{\mathbf{x} \in \mathcal{X}} f(\mathbf{x}, W), \quad (1)$$

where \mathcal{X} is the Spark configuration search space and $f(\mathbf{x}, W)$ is the performance (in our case, latency) of W under configuration \mathbf{x} .

3.3 Bayesian Optimization Framework

Bayesian optimization (BO) [3, 12, 44] is a popular algorithm framework that solves black-box problems with a costly objective function. Typically, BO loops over the following three main steps: (1) it fits a *surrogate model* M based on observed configurations $D = \{(\mathbf{x}_1, y_1), \dots, (\mathbf{x}_{n-1}, y_{n-1})\}$, where \mathbf{x}_i is the i^{th} configuration and y_i is the corresponding observed performance; (2) with the surrogate model M , BO chooses the next configuration to evaluate by maximizing the *acquisition function* $\mathbf{x}_n = \arg \max_{\mathbf{x} \in \mathcal{X}} \alpha(\mathbf{x}; M)$; (3) BO evaluates the configuration \mathbf{x}_n to obtain its performance y_n and augments the observations by $D = D \cup \{(\mathbf{x}_n, y_n)\}$.

Surrogate. We apply the Probabilistic Random Forest [12] as the surrogate. Compared to alternatives, it has lower time complexity and shows better empirical results in real-world scenarios [62].

Acquisition function. We apply the Expected Improvement (EI) [17] function to estimate the performance improvement of an unseen configuration \mathbf{x} . Given the marginal predictive mean $\mu(\mathbf{x})$ and variance $\sigma^2(\mathbf{x})$ from the surrogate M , the EI function is defined as the expected improvement over the best performance found,

Algorithm 1 Pseudo code for Hyperband.

Input: Maximum amount of resource that can be allocated to a single configuration R , discard proportion η , search space \mathcal{X} .

- 1: Initialize $s_{\max} = \lfloor \log_{\eta}(R) \rfloor$, $B = (s_{\max} + 1)R$.
 - 2: **for** $s \in \{s_{\max}, s_{\max} - 1, \dots, 0\}$ **do**
 - 3: $n_1 = \left\lceil \frac{B}{R} \frac{\eta^s}{s+1} \right\rceil$, $r_1 = R\eta^{-s}$.
 - 4: Sample n_1 configurations from \mathcal{X} randomly.
 - 5: Execute the SH with the n_1 configurations and r_1 as input (the inner loop).
 - 6: **end for**
 - 7: **return** the configuration with the best evaluation result.
-

Table 1: The values of n_i and r_i in the HB evaluations, where $R = 27$ and $\eta = 3$. Each column shows an inner loop (SHA process). The pair (n_i, r_i) in each cell indicates n_i configuration evaluations with r_i units of training resources.

i	$s = 3$		$s = 2$		$s = 1$		$s = 0$	
	n_i	r_i	n_i	r_i	n_i	r_i	n_i	r_i
1	27	1	12	3	6	9	4	27
2	9	3	4	9	2	27		
3	3	9	1	27				
4	1	27						

i.e., $EI(x) = \int_{-\infty}^{\infty} \max(y - y^*, 0) p_M(y|x) dy$, where y^* is the best performance observed so far.

Initialization. Before training the surrogate with sufficient observations, we default to initializing BO by sampling configurations using Latin Hypercube Sampling [33] from the search space.

3.4 Hyperband Framework

To address this challenge, Hyperband (HB) [27] accelerates evaluations by halting poorly performing configurations early. The HB framework consists of three key components: a fidelity partitioning strategy, and nested outer and inner loops responsible for scheduling multi-fidelity evaluations.

Fidelity partition determines how to allocate $r (r \leq R)$ units of resources to evaluate a configuration when the maximum resource is R . As existing methods are particularly applied in automated machine learning (AutoML) and neural architecture search (NAS), the typical approaches involve either training for fewer epochs [7, 16, 30] or using a subset of the dataset [20, 30, 31].

Inner loop: successive halving (SH). Given a type of resource partition (e.g., number of epochs or dataset size), HB initially evaluates n_1 configurations with each using r_1 units of resources, ranking them by performance. HB then continues with only the top η^{-1} configurations using η times more resources (typically $\eta = 3$), i.e., $n_2 = n_1 \times \eta^{-1}$ and $r_2 = r_1 \times \eta$. This process repeats until the maximum training resource R is reached, i.e., $r_i = R$.

Outer loop: grid search of n_1 and r_1 . With a fixed budget \mathcal{B} , n_1 and r_1 must be carefully selected. HB tackles this by performing a grid search over feasible values of n_1 and r_1 . Algorithm 1 demonstrates the enumeration of n_1 and r_1 . Table 1 lists the number of evaluations and their corresponding training resources in one HB iteration, where each column corresponds to one inner loop.

4 OVERVIEW

In this section, we present an overview of our efficient multi-fidelity Spark SQL configuration tuning system, dubbed MFTune, and then introduce how we facilitate knowledge transfer across components through similar tasks identification.

4.1 System Overview

Figure 2 provides an overview of MFTune’s framework, which consists of five components: 1) The MFTune controller interacts with users and the Spark SQL server, and controls the tuning process. 2) The knowledge database stores both observations and meta-features from the current task as well as historical tasks, which are used to identify similarities between tasks. 3) The search space optimizer identifies an optimal subspace from the original search space. 4) The configuration generator suggests a set of promising configurations. 5) The multi-fidelity optimizer is responsible for partitioning and arranging the evaluations of varying fidelity.

Workflow. To initiate a tuning task, the user first specifies the tuning objective, the tuning budget, and uploads the target workload to the controller. An iterative tuning workflow is then activated. During each iteration, ① the **knowledge database** first calculates the similarity between source tasks and the current task based on meta-features and historical observations, and delivers similar source tasks to other components. ② The **search space optimizer** then compresses the original search space based on the observations of similar tasks, encompassing both the selection of important knobs and the narrowing of their value ranges. ③ After that, the **configuration generator** samples a batch of promising configurations from the compressed search space. Among these, a subset is sourced from top-performing configurations of similar tasks to warm-start the search, while the remainder are obtained via Bayesian optimization with a combined surrogate model to fit all the available observations. ④ Upon receiving the candidate configurations, the **multi-fidelity optimizer** evaluates and filters them iteratively. If no fidelity partition strategy has yet been determined, it first derives one based on similar tasks (this partitioning is done only once). It then begins evaluation at the lowest fidelity, progressively eliminating suboptimal configurations and increasing fidelity in each round until the original workload is reached. ⑤ Finally, the **MFTune controller** aggregates all execution results from the current iteration and stores them in the knowledge database. Based on resource limits such as maximum optimization time or iterations specified by users, once the tuning process is complete, MFTune identifies the optimal configuration from the history of the current task and recommends it to the user.

4.2 Similarity Identification

A Spark SQL tuning system can accumulate a wealth of historical tasks as it performs tuning tasks on different workloads. These previous tasks can offer valuable insights for the current tuning. For instance, similar query workloads running on different hardware or with varying data scales may share critical queries, aiding us in partitioning low-fidelity workloads. Even for different query workloads, they may still assist in identifying the promising region within the search space [42, 65]. However, as previous studies have shown, transferring knowledge from dissimilar tasks can lead to

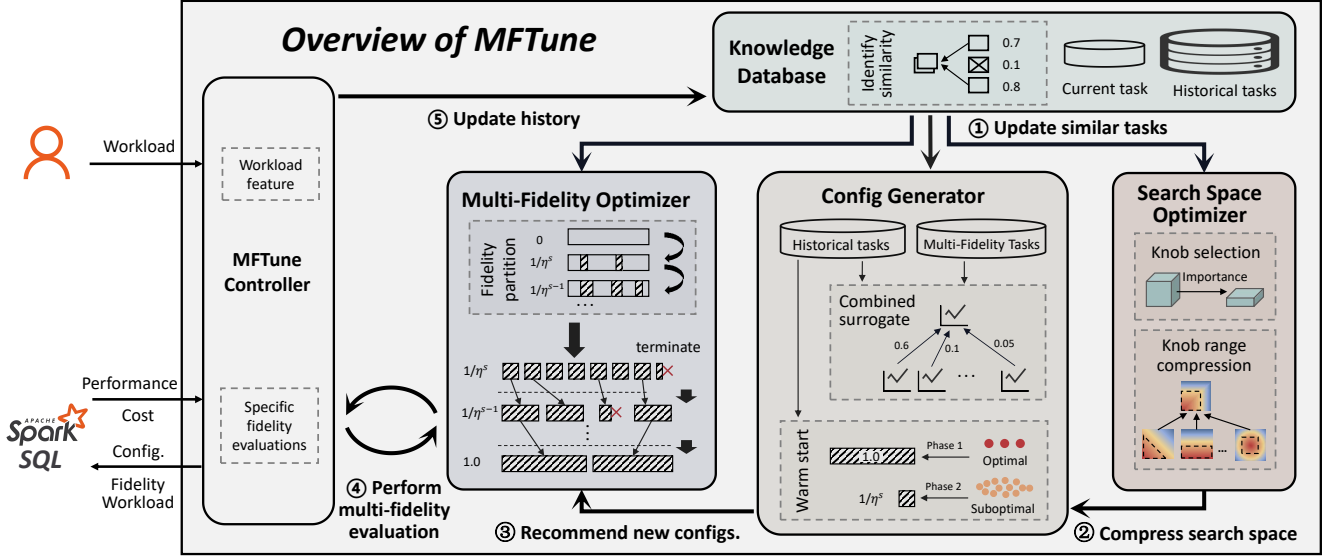


Figure 2: Overview: architecture and workflow of MFTune.

negative impacts [43]. Hence, for a given target task, it is essential to identify similar tasks to ensure safe transfer.

To quantify the similarity between a source task and the target task, it is common to consider whether the two tasks have similar performance rankings for different configurations [46, 63]. Given the observations \mathcal{D}_T of the target task—consisting of configuration-performance pairs—if a surrogate model of the source task can correctly predict the relative performance between configurations, the source task is considered similar to the target. Therefore, for the target task and a source task, we measure their similarity using the Kendall-tau coefficient based on the target observations. Formally, the similarity $S(i, T)$ between the i -th source task and the target task is defined as:

$$S(i, T) = \text{KendallTau}^{\mathcal{D}_T}(M_i, Y) \quad (2)$$

where M_i is the BO surrogate model trained on observations \mathcal{D}_i of the i -th source task, and $\text{KendallTau}^{\mathcal{D}_T}(M_i, Y)$ is the Kendall-tau coefficient between the predictive values and the ground truth performance on the current observations \mathcal{D}_T .

Warm-starting through prediction. However, a limitation of the above similarity metric has been overlooked in existing works. The reliability of the measure in Equation 2 is reduced when the size of \mathcal{D}_T is small. This results in inaccurate or highly fluctuating similarity measures during the initial iterations of the tuning task. To mitigate this disadvantage, we extend Rover [42] to warm-start similarity identification during the initial phase. We first extract the feature vectors of a Spark SQL workload from SparkEventLog under the default configuration, in which Spark event information is logged during the execution of each query. The feature vectors of all the queries are then averaged to form the meta-feature of the tuning task. A LightGBM regression model, which takes two meta-features as inputs, is fitted to predict the pair-wise similarity between tuning tasks. The training data is derived from the tuning history in the knowledge database. The similarity label between the i -th and

j -th task is defined as $\text{KendallTau}^{\mathcal{D}_{rand}}(M_i, M_j)$, the Kendall-tau coefficient of surrogate predictions on random configurations. After training the regression model, when a new tuning task starts, we compute its similarity with all historical tasks using meta-features.

Transition mechanism. As for the transition from predicted similarity to Kendall-tau coefficient similarity, the key insight is that when the observations of the target task are sufficient, reducing the influence of randomness on the calculations, Equation 2 becomes more reliable compared to predicted values. Therefore, the transition is implemented when the majority of source tasks satisfy that the p -value of the Kendall-tau coefficient is less than 0.05. As the number of target observations grows, the similarity measure will increasingly approximate the ground-truth similarity.

Weighting based on similarity. After obtaining the similarities of all source tasks, we first filter out source tasks with negative similarity, as they provide less utility for the target task than a random guess. Subsequently, the similarities are converted into weights to facilitate the transfer of knowledge. The weight assigned to the i -th task is proportional to its similarity with the target task, i.e., $w_i = S(i, T) / \sum_j S(j, T)$. For generality, MFTune also assigns a weight to the target tuning task. To achieve that, we measure its generalization ability on unseen configurations using the out-of-sample Kendall-tau coefficient. Specifically, we perform cross-validation on \mathcal{D}_T . When predicting the performance of configurations in each fold, the surrogate model is trained using the data from the remaining folds. Similarly, the generalization ability can be computed using Equation 2 and then converted into weights.

5 CONFIGURATION SPACE COMPRESSION

Facing the challenge of the huge search space, existing works manage to compress the original space into a compact and promising one, thereby reducing resource waste in exploring suboptimal regions and enhancing tuning efficiency [18, 54, 65]. The compression of search space consists of two aspects: reducing the number of

knobs and narrowing the value range of each knob. As for the number of knobs, one kind of method utilizes sensitivity analysis algorithms such as Lasso [48] and SHAP [32] to identify knobs that significantly impact performance [8, 29, 56]. Another kind of methods adopts knob-dimensional projection-based methods like HeSBO [24] and ALEBO [35] to conduct BO in a low-dimensional space [18, 54]. All the above methods require a significant hyperparameter for setting the number of remaining knobs. As for the value range, the typical strategy is to transfer promising regions from similar tasks [46, 65]. However, they often rely solely on the boundary values of discrete historical configurations to define the range. This can result in overly large retained ranges susceptible to outliers or the loss of better values due to insufficient exploration in historical configurations. Therefore, how to effectively compress the search space remains underexplored. Next, we explain (1) how we extract promising regions from source tasks and (2) how we combine them to generate the target search space, including the important knobs and their value ranges.

5.1 Promising Regions Extraction

MFTune first extracts the promising discretized region for each knob from similar source tasks. Specifically, for the observations \mathcal{D}_i of the i -th source task, we calculate the median performance of all recorded configurations, denoted as f_{median}^i . We then define the promising configurations set G_i as the set of configurations with performance exceeding the median, i.e., $G_i = \{\mathbf{x} \in \mathcal{D}_i \mid f^i(\mathbf{x}) < f_{\text{median}}^i\}$, where $f^i(\mathbf{x})$ is the performance of \mathbf{x} in the source task.

Although all configurations in G_i are promising, it cannot be guaranteed that every knob value in each configuration contributes positively to the performance. Therefore, we employ SHAP to analyze the importance of each knob. Specifically, SHAP computes the impact of each knob value in every configuration within G_i . A positive SHAP value indicates that the knob value increases latency and degrades performance, whereas a negative SHAP value indicates that it decreases latency and improves performance. Based on this, we define the promising value set for each knob as the set of knob values with a negative SHAP value (assuming a minimization objective). Specifically, for a knob k_j , its promising value set P_j^i in this source task is defined as:

$$P_j^i = \left\{ (\mathbf{x}[k_j], v(\mathbf{x})) \mid \mathbf{x} \in G_i \text{ and } \text{SHAP}(\mathbf{x}[k_j]) < 0 \right\},$$

$$v(\mathbf{x}) = w_i \cdot \frac{f_{\text{median}}^i - f^i(\mathbf{x})}{f_{\text{median}}^i}, \quad (3)$$

where $\mathbf{x}[k_j]$ denotes the value of k_j in configuration \mathbf{x} and $v(\mathbf{x})$ is the weight of this value. We define $v(\mathbf{x})$ as the product of the source task's weight w_i and the performance improvement rate of the configuration compared to f_{median}^i . In other words, higher weights are assigned to knob values from better-performing configurations in more similar tasks. If a knob only contains positive SHAP values, tuning this knob will not yield any performance improvement. Accordingly, the promising region for it is an empty set \emptyset .

5.2 Density Modeling and Target Search Space

Given the promising discretized regions extracted from each source task, the final step is to generate the target search space. Assuming there are K source tasks, for each knob k_j , if the majority of tasks

have P_j^i as an empty set, i.e., $\sum_{i=1}^K w_i \cdot \mathbb{I}(P_j^i = \emptyset) > 0.5$, it indicates that this knob is generally not worth tuning and can be removed from the search space. Otherwise, we construct the final promising value set P_j for k_j by taking the union of the promising value sets from all source tasks, i.e., $P_j = \bigcup_{i=1}^K P_j^i$. Instead of directly using the boundaries of the discrete values, we model the density of optimal values for each knob to identify specific regions where promising configurations are concentrated.

To model the density of continuous knobs, we employ the **Kernel Density Estimation (KDE)** function, a non-parametric method used to estimate the probability density function of a random variable [37]. Specifically, for each continuous knob, we collect the values corresponding to promising configurations and use these samples, along with their associated weights, to construct a weighted density curve. The weighted KDE function is defined as:

$$\hat{g}(x) = \frac{1}{h \cdot \sum_{(\theta, v) \in P_j} v} \sum_{(\theta, v) \in P_j} v \cdot K\left(\frac{x - \theta}{h}\right), \quad (4)$$

where each (θ, v) pair represents a value in the promising value sets and its associated weight, h denotes the bandwidth controlling the smoothness of the density estimation and is determined according to Silverman's rule of thumb, and $K(\cdot)$ denotes the kernel function, typically a Gaussian kernel. The inclusion of weights ensures that promising configurations exert a finer-grained on the density curve, providing a smoother and data-driven representation of the value set in contrast to the discrete boundaries used in [46, 65].

To extract the region with the highest density from $\hat{g}(x)$ and compress the range of values, we formalize this task as an optimization problem. First, we define a cumulative density threshold $\alpha \in [0, 1]$, which represents the desired proportion of the total probability mass to be covered. Assume that the original range of k_j is $R_j \subset \mathbb{R}$. The goal is to identify a sub-region within R_j , denoted as R_j^{opt} , that minimizes the total length of the region while capturing at least α of the total probability mass:

$$\min_{R_j^{\text{opt}} \subset R_j} |R_j^{\text{opt}}| \quad \text{s.t.} \quad \int_{R_j^{\text{opt}}} \hat{g}(x) dx \geq \alpha, \quad (5)$$

To solve this problem, the values of the kernel density estimation function $\hat{g}(x)$ can be sorted in descending order, and the density values are accumulated until the cumulative density reaches or exceeds the threshold α . Finally, the smallest region R_j^{opt} satisfying the condition is determined.

To process categorical knobs, we redefine Equation 4 in a discrete form to build the density function, as follows:

$$\hat{g}(x) = \frac{1}{\sum_{(\theta, v) \in P_j} v} \sum_{(\theta, v) \in P_j} v \cdot \mathbb{I}(x = \theta), \quad (6)$$

where $\mathbb{I}(x = \theta)$ is the indicator function. The subsequent solution process is consistent with that for continuous parameters, ensuring a unified framework for both categorical and continuous knobs.

Compared to existing methods, our approach offers three advantages: 1) It does not require a hyperparameter to set the number of important knobs. By integrating the promising regions of similar tasks, it simultaneously achieves knob selection and range compression. 2) With density modeling, we can identify specific regions where promising configurations are concentrated. On the one hand,

this avoids the interference of outliers. On the other hand, it has the potential to include regions near historical points that may also be promising. 3) As the similarity measure of source tasks gradually approaches the ground-truth similarity, our search space adapts dynamically during the tuning process.

6 MULTI-FIDELITY OPTIMIZATION

In this section, we propose applying multi-fidelity optimization (MFO) to Spark SQL for efficient configuration tuning. Specifically, we introduce how MFTune (1) partitions fidelity levels, (2) generates candidate configurations, and (3) performs the MFO process.

6.1 Fidelity Partition

As introduced in Section 3.4, fidelity partition plays a fundamental role in multi-fidelity optimization. Assuming that evaluating a configuration on the original workload represents full-fidelity evaluation (e.g., running 99 queries on 1TB of data), we define a δ -fidelity evaluation ($0 < \delta \leq 1$) as evaluating a configuration using δ fraction of the resources costed for full fidelity (e.g., elapsed time or memory consumption). To ensure effective optimization, low-fidelity evaluations should preserve the relative ranking of configurations as much as possible to avoid discarding those that perform well under full fidelity. Existing work often uses smaller datasets or fewer training epochs to define low fidelity, which are either unreliable or entirely unsuitable for Spark SQL. Therefore, we propose partitioning low fidelity in Spark SQL by selecting a subset of queries. Compared to alternatives, it has three advantages: 1) Query selecting preserves the diversity of the workload while maintaining critical performance bottlenecks that are typically lost when data volume is reduced. 2) It does not require the additional overhead like generating smaller datasets. 3) A carefully selected subset of queries can achieve higher representativeness with full-fidelity evaluation compared to other fixed strategies.

Assume that the original workload consists of a set of queries $Q = \{q_1, q_2, \dots, q_m\}$, the goal of the fidelity partition is to identify a representative subset of queries from Q , such that the subset $Q_\delta \subseteq Q$ achieves high evaluation correlation with the results of the full query set, while incurring a lower computational cost. Specifically, for δ -fidelity evaluation, the selected subset Q_δ should satisfy a cost constraint $\text{Cost}(Q_\delta) \leq \delta \cdot \text{Cost}(Q)$, where $\delta \in (0, 1]$ represents the desired cost reduction factor. The optimization problem can be formally defined as:

$$\max_{Q_\delta \subseteq Q} \tau(Q_\delta, Q) \quad \text{s.t.} \quad \text{Cost}(Q_\delta) \leq \delta \cdot \text{Cost}(Q), \quad (7)$$

where $\tau(Q_\delta, Q)$ measures the correlation score between the subset Q_δ and Q . To calculate this, we can collect the performance of each query across multiple configurations for the current task. The correlation can then be calculated using rank-based metrics, such as the Kendall-tau coefficient, as we focus on the ability of low-fidelity evaluations to correctly rank configurations rather than predict exact performance values.

However, collecting sufficient evaluation data under full-fidelity evaluation incurs significant computational overhead. To address this, knowledge can be transferred from source tasks where the query workloads were the same but evaluated under different conditions. Such scenarios are common in practice. For example, the

Algorithm 2 Greedy Solution for Query Subset Selection

Input: Full query set $Q = \{q_1, q_2, \dots, q_m\}$, fidelity δ , Observations from all source tasks $\{\mathcal{D}_1, \mathcal{D}_2, \dots, \mathcal{D}_{K'}\}$

Output: Optimal subset Q_δ

- 1: Initialize $Q_\delta \leftarrow \emptyset$ and cost ratio $r \leftarrow 0$ {Start with empty}
 - 2: Compute the weighted average cost ratio of all queries: $c(q) = \frac{\sum_{\mathbf{x} \in C_i} c_{q,\mathbf{x}}}{\sum_{q_j \in Q} \sum_{\mathbf{x} \in C_i} c_{q_j,\mathbf{x}}}$.
 - 3: **while** True **do**
 - 4: $q^* \leftarrow \arg \max_{q \in Q \setminus Q_\delta} \hat{\tau}$, where $\hat{\tau} = \tau(Q_\delta \cup \{q\}, Q)$ and $r + c(q) \leq \delta$
 - 5: **if** q^* is null **then**
 - 6: **break**
 - 7: **end if**
 - 8: $Q_\delta \leftarrow Q_\delta \cup \{q^*\}$, $r \leftarrow r + c(q^*)$
 - 9: **end while**
 - 10: **return** Q_δ
-

same query set might be executed on different datasets or on different hardware, providing valuable insights to guide the subset selection without requiring extensive new evaluations. Moreover, transferring information about critical queries from similar source tasks is logical. Task similarity implies that the relative performance of different configurations remains consistent across tasks. This consistency indicates shared performance bottlenecks, meaning that queries crucial in one task, susceptible to these bottlenecks, are likely important in another. Therefore, we first select source tasks where the query set is identical to the current task. Then for the i -th source task, let $\mathcal{D}_i = \{(\mathbf{x}, \mathbf{p}_x, \mathbf{c}_x)_{\mathbf{x} \in C_i}\}$ represent the observation data, where C_i is the set of configurations evaluated in the i -th task, $\mathbf{p}_x = [p_{q_1,\mathbf{x}}, p_{q_2,\mathbf{x}}, \dots, p_{q_m,\mathbf{x}}]$ is a vector containing the performance of configuration \mathbf{x} across all queries in the full query set, and $\mathbf{c}_x = [c_{q_1,\mathbf{x}}, c_{q_2,\mathbf{x}}, \dots, c_{q_m,\mathbf{x}}]$ contains the cost of configuration \mathbf{x} across all queries. Typically, there is an aggregation function $\text{Agg}(\cdot)$ that combines the performance of individual queries within a query set into an overall performance for the multi-query workload. In our scenario, the performance metric is latency, and the aggregation function is defined as the summation of latency values, i.e., $\text{Agg}(Q_{\text{var}}, \mathbf{p}_x) = \sum_{q \in Q_{\text{var}}} p_{q,\mathbf{x}}$, where Q_{var} is a query set. Based on this, the correlation score of Q_δ in the i -th source task is:

$$\begin{aligned} \tau_i(Q_\delta, Q) &= \text{KendallTau}(A_i^{Q_\delta}, A_i^Q), \\ A_i^{Q_{\text{var}}} &= \{\text{Agg}(Q_{\text{var}}, \mathbf{p}_x) \mid \mathbf{x} \in C_i\}. \end{aligned} \quad (8)$$

After that, the overall correlation score is defined as the weighted sum of all source task scores, i.e., $\tau(Q_\delta, Q) = \sum_i w_i \tau_i(Q_\delta, Q)$.

Greedy solution. We observe that Problem 7 has transformed into a combinatorial optimization problem with a well-defined expression. To approximate its solution, we propose a greedy algorithm that starts with an empty set and iteratively adds the query that maximizes the correlation score, until the average cost of the queries in Q_δ exceeds δ fraction of the full query set. Algorithm 2 presents the pseudo code of the greedy algorithm.

6.2 Efficient Candidate Generation

MFO requires a set of candidate configurations for iterative filtering. In this subsection, we introduce the method in the configuration generator to recommend a set of promising configurations.

Inspired by BOHB [7], we employ Bayesian Optimization (BO) [12] for configuration recommendation, as it more effectively balances exploration and exploitation than Hyperband’s random sampling. However, BO often struggles with accuracy during the early stages of optimization due to sparse observations. To address this ‘cold-start’ issue, prior works integrate surrogate models from historical tasks to guide the search [29, 63]. In the scenario of MFO, MFES [31] builds a surrogate for the observations of each evaluation fidelity and combines them. MFTune integrates the two aforementioned approaches by treating both historical tasks and tasks at each fidelity level as source tasks. It computes their weights using the method described in Section 4.2 and combines their surrogate models accordingly. To account for the varying scales of surrogate outputs across different source tasks, we aggregate the ranks of the acquisition function scores from each surrogate model. Given a set of candidate configurations through sampling and mutation, we denote the ranking value of the configuration \mathbf{x} based on surrogate M_i of the i -th source task as $R_i(\mathbf{x})$. The combined ranking of \mathbf{x} is computed as $R(\mathbf{x}) = \sum_i w_i R_i(\mathbf{x})$. Finally, MFTune recommends the top- n configurations, as specified by the outer loop of MFO.

Two-phase warm start. To further improve the tuning efficiency, many works select configurations from similar tasks as initial configurations for warm start [26, 29, 43]. However, they face a trade-off between exploration and exploitation: if the number of warm-start configurations is small, historical tasks may not be sufficiently utilized; if the number is large, it occupies much exploration budget for the current task. To overcome this, we propose a two-phase warm start strategy. Phase 1 is similar to existing methods. We select the best configuration from the best similar historical tasks and directly perform full-fidelity evaluation at the beginning of the tuning process. After this, MFTune begins MFO and transitions to the Phase 2 warm start. Specifically, we select all the remaining configurations from each source task that outperform the median performance (i.e., G_i defined in Section 5.1), and aggregate them into a warm start configuration set $G_{ws} = \bigcup_{i=1}^K G_i$. We then rank the configurations in G_{ws} according to $v(\cdot)$ defined in Equation 3, which means stronger configurations from more similar tasks are assigned higher priority. At the start of each inner loop of MFO, with the exception of those consisting solely of full-fidelity validation, we sequentially recommend a few configurations from G_{ws} as candidate configurations, while the remaining candidates are suggested by BO. The number of configurations recommended from G_{ws} is set to match the number of fully evaluated configurations in each inner loop, ensuring that promising configurations do not eliminate each other. Compared to existing strategies, warm start in MFTune has two strengths: 1) We adopt two levels of utilization for configurations with varying priorities. 2) We achieve a balance between exploration and exploitation by leveraging historical task observations to the fullest extent without hindering exploration. As the vast majority of candidates are still recommended by BO, and suboptimal warm-start configurations are filtered out during low-fidelity evaluation without wasting excessive resources.

6.3 Multi-Fidelity Optimization Process

In this subsection, we discuss how MFTune combines the above strategies to perform multi-fidelity optimization.

Before the start of each inner loop in MFO, MFTune utilizes Algorithm 2 to determine the query subsets to be used for each fidelity evaluation. The configuration generator then leverages warm start and the combined surrogate to recommend a set of candidate configurations. After that, MFTune adopts the Hyperband framework to perform MFO. As illustrated in Section 3.4, due to the heavy-tailed cost distributions across various configurations, MFTune adopts an early stopping mechanism for each fidelity. Specifically, if the cost of the current evaluation exceeds the median cost of all historical evaluations at the same fidelity, the evaluation is terminated to prevent poor configurations from consuming excessive resources.

Tuning across diverse historical task scenarios. Ideally, the knowledge database stores history from past tuning tasks, including some with query sets identical to the current task. On one hand, if no historical tasks share the same query set, MFTune will start optimization with full-fidelity evaluation only. Subsequently, MFTune transitions to multi-fidelity optimization (MFO) in two steps: 1) As more observations are gathered, the transition mechanism outlined in Section 4.2 automatically determines when to apply the Kendall-tau coefficient similarity, allowing the current task to act as a source task for fidelity partitioning. 2) For δ -fidelity, we use the score defined by Equation 8 on the current task as the criterion for fidelity partition, e.g., $\tau_T(Q_\delta, Q)$. And we can execute fidelity partition with Algorithm 2. In this case, the space compression and modules in the configuration generator remain unaffected. On the other hand, in the worst case that no historical task data is available, MFTune will initially fall back to vanilla BO. However, with more observations collected, the transition mechanism in Section 4.2 will automatically determine when the current task can serve as a source task, enabling space compression. Similarly, MFO will also be automatically enabled afterward. To sum up, under different scenarios, the components of MFTune can adaptively function to enhance tuning efficiency.

7 EXPERIMENTAL EVALUATION

7.1 Experiment Setup

Baselines. For end-to-end comparison, we compare MFTune with five SOTA tuning methods. — *Two approaches that do not rely on historical data:* 1) *LOCAT* [56], a method that gradually identifies the important knobs to reduce the search space. 2) *TopTune* [54], a DBMS tuning method that utilizes a knob-dimensional projection strategy to reduce the exploration domain and tunes the categorical and continuous knobs alternately. — *Three approaches that rely on historical data:* 3) *Tuneful* [8], a method that explores significant parameters and applies a multi-task GP to use the most similar previous task. 4) *Rover* [42], a system that utilizes the historical knowledge by adaptive weight for similar historical workloads. 5) *LOFTune* [26], a system that identifies similar workloads with a multi-task SQL representation model and uses a workload-aware performance simulator to fit all historical data.

Benchmarks. We select two typical benchmarks for evaluation following literature [1, 8, 26]. 1) *TPC-H*, a decision support benchmark with 22 queries designed to simulate business-oriented

Table 2: Hardware Scenarios

Scenario	A	B	C	D	E	F	G	H
Node	3	3	3	3	2	2	2	2
CPU (cores)	64	32	32	64	64	32	32	64
RAM (GB)	256	128	256	128	256	128	256	128

ad-hoc queries and concurrent data modifications. 2) *TPC-DS*, a comprehensive benchmark with 99 queries aimed at evaluating decision support systems. We utilize two data sizes (100GB and 600GB) for both TPC-H and TPC-DS benchmarks, resulting in four workloads based on the combination of benchmarks and data sizes.

Environment. We conducted the experiments using Spark 3.4.4 on the OpenEuler 22.03 operating system [36]. To simulate tuning and knowledge transfer across different hardware environments, experiments were conducted on eight hardware scenarios, varying in node count (2 or 3), CPU cores (32 or 64), and memory (128GB or 256GB), as shown in Table 2. Unless otherwise specified, Scenario A serves as the default hardware environment for our evaluations.

Historical data. We collect task meta-features and observation histories of 32 distinct tuning tasks, derived from the combination of benchmarks, data sizes, and eight hardware scenarios. Each meta-feature is a 34-d vector extracted from SparkEventLog as shown in Section 4.2. Observation histories were prepared by applying vanilla Bayesian Optimization (BO) [12] and collecting 50 observations per task. To evaluate the generalizability, we conduct our experiments under five settings: 1) *original setting*, 2) *cross-benchmark transfer setting*, 3) *cold-start setting*, 4) *varying data size setting*, 5) *varying hardware setting*. Under the *original setting*, we adopt a leave-one-out pattern, using historical data from 31 tasks that differ from the target task. In the *cross-benchmark transfer setting*, we hold out historical data from the same benchmark and use only the remaining 16 histories. The *cold-start setting* requires the optimizer to initialize the search purely from scratch with no access to historical data. The remaining two settings follow a similar pattern with 2). Unless otherwise specified, we adopt the original setting for evaluation.

Tuning Setting. 1) *Optimization target*: In all experiments, we optimize the total latency (i.e., the sum of all query times) of the target Spark SQL workload, and use elapsed time as the cost metric for fidelity partitioning. 2) *Search space*: We extend the search space in Tuneful [8] to include 60 parameters that influence the application performance. More details are available in the repository <https://github.com/Elubrazione/MFTune>. 3) *Tuning budget*: For each target tuning task except for the cold-start setting, we run each tuning method for 48 hours and record the best-observed performance of the configurations they suggest and evaluate. 4) *Implementation details*: MFTune implements BO based on OpenBox [15], a toolkit for black-box optimization. We set the cumulative density threshold α to 0.65. As for the MFO, we set the reduction factor $\eta = 3$ and the maximum resource $R = 9$ as detailed in Section 3.4. This configuration generates two low-fidelity proxy levels, corresponding to 1/9 and 1/3 of the full resources, respectively. The other baselines are implemented following their original papers.

7.2 Results under Original Setting

In this section, we evaluate the performance of MFTune and the baselines on the TPC-H and TPC-DS under the original setting.

These experiments are conducted on Hardware Scenario A in Table 2 with a data scale of 600GB. We adopt a leave-one-out pattern, utilizing historical data from 31 distinct tasks. Under this setting, the historical repository contains source tasks from the same benchmark as the target, providing the most abundant prior knowledge. Consequently, MFTune can perform fidelity partitioning and MFO at the very beginning of the tuning process.

The experimental results are illustrated in Figure 3a and 3d, from which we can draw the following conclusions: 1) methods that leverage historical data (MFTune, Tuneful, Rover, and LOFTune) generally exhibit superior performance and faster optimization progress compared to those that do not rely on history (LOCAT and TopTune), demonstrating that historical knowledge from related tasks significantly accelerates the search for high-quality configurations in complex Spark SQL environments. 2) Among the approaches utilizing historical knowledge, MFTune demonstrates a markedly superior convergence profile. While LOFTune initially achieves rapid latency reduction through its warm-start mechanism, its utilization of historical tasks is restricted to the initialization phase. Such insufficient exploitation of prior knowledge causes its performance to stagnate, allowing Rover and Tuneful to eventually surpass it. Tuneful exhibits faster early-stage convergence compared to Rover as it benefits from both space compression and transfer learning, whereas Rover lacks a mechanism for domain reduction. Furthermore, although these baselines leverage transfer learning to accelerate convergence, their exclusive reliance on full-fidelity evaluations inevitably leads to time-consuming explorations of poor configurations. By contrast, MFTune employs multi-fidelity optimization to rapidly filter out these suboptimal configurations, sustaining a continuous and steep reduction in latency throughout the process by synergizing MFO with space compression and transfer learning. 3) MFTune yields the best final tuning results across both benchmarks. Specifically, compared to all five SOTA baselines, MFTune reduces execution latency of Spark SQL ranging from 25.9% to 43.1% on TPC-H and 37.8% to 63.1% on TPC-DS.

7.3 Evaluation on Generalization

This subsection examines the generalization of MFTune, assessing its adaptability and performance in diverse scenarios.

7.3.1 Results in Cross-Benchmark Transfer. In this section, we evaluate the robustness of MFTune under a cross-benchmark transfer setting to assess its generalization capabilities across distinct workloads. In this scenario, we compare MFTune against the three baselines that utilize historical data (Tuneful, Rover, and LOFTune), which are the top-3 baselines in the original setting. Following the experimental setup, when TPC-H is the target benchmark, we provide the framework with 16 source tasks exclusively from TPC-DS, and vice versa. As discussed in Section 6.3, since the historical repository lacks same-benchmark data, MFTune cannot perform fidelity partitioning at the outset. Consequently, the framework initially relies on transfer learning and search space compression while executing full-fidelity evaluations. Once sufficient observations are accumulated, MFTune dynamically partitions the target workload into low-fidelity proxies and activates multi-fidelity optimization.

The experimental results are illustrated in Figure 3b and 3e. We can observe that the activation of multi-fidelity optimization is

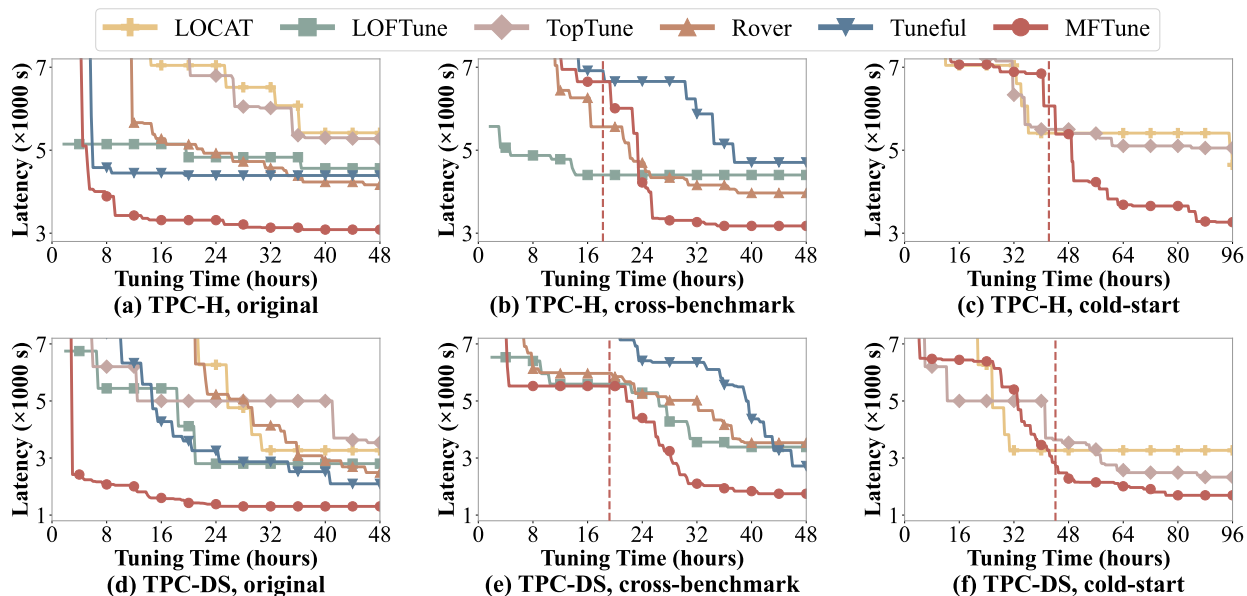


Figure 3: Comparison of tuning performance over time across six scenarios, encompassing two benchmarks and three experimental settings. Each curve represents the average cumulative best latency across three independent experimental runs of a method. The vertical red dashed line indicates the time point MFTune activates multi-fidelity optimization when fidelity partitioning is not applicable at the beginning.

notably delayed compared to the original setting. The vertical red dashed line marks the specific time point MFTune enables this feature once fidelity partitioning becomes applicable with sufficient observations. Importantly, following this activation, the performance gap between MFTune and the baselines widens significantly as low-fidelity proxies enable high-frequency explorations beyond the reach of full-fidelity methods. Finally, MFTune also yields the best tuning results in this scenario. Specifically, compared to the baselines, MFTune achieves a latency reduction ranging from 20.0% to 32.5% on TPC-H and 35.7% to 50.6% on TPC-DS, proving its superior adaptability to unfamiliar workloads.

7.3.2 Results without Historical Data. To further evaluate the robustness of MFTune in extreme scenarios, we conduct experiments under a cold-start setting where no historical data is available. In this subsection, we compare MFTune against TopTune and LOCAT, the two baselines that do not rely on historical knowledge. Unlike the previous settings, the tuning budget here is extended to 96 hours to allow for sufficient exploration from scratch on the 600GB data scale. As detailed in Section 6.3, since there are no historical tasks to leverage, MFTune initially degrades to a vanilla BO. As the process continues and online observations accumulate, the system automatically enables space compression and MFO.

Figure 3c and 3f illustrate the experimental results for TPC-H and TPC-DS, respectively. During the initial tuning phase, MFTune exhibits a similar convergence trend to the baselines while gathering the necessary observations. However, once MFO is activated (marked by the vertical red dashed line), the convergence speed increases significantly, demonstrating that MFTune can successfully identify and utilize low-fidelity proxies online even without prior

history. Eventually, MFTune achieves a much lower final latency compared to TopTune and LOCAT, which remain limited by the high temporal cost of performing exclusive full-fidelity evaluations. Specifically, MFTune outperforms LOCAT and TopTune by 29.7% and 35.4% on TPC-H, and by 48.2% and 27.4% on TPC-DS.

7.3.3 Results with Varying Data Size and Hardware. In this subsection, we evaluate the generalization capabilities of MFTune on TPC-H under varying data size settings and varying hardware settings. In Figure 4a, we conduct cross-scale transfers between 100GB and 600GB data sizes on Hardware A. When the target task is set to 600GB, we utilize 16 historical tasks from the 100GB setting as source tasks, and vice versa. Furthermore, Figure 4b illustrates the generalization across different hardware configurations, including node counts, CPU cores, and RAM capacities. In a typical scenario such as the 2 → 3 nodes transition, we select Hardware A (600GB) as the target task and leverage 16 source tasks from the 2-node environments (Hardware E, F, G, H) as the historical dataset.

The experimental results demonstrate the superior robustness of MFTune compared to existing transfer-learning-based methods. MFTune consistently achieves the highest speedup relative to the default configuration across all tested scenarios. Notably, it reaches a peak speedup of 3.96x in the 600 → 100 GB data size transfer. In hardware-shifting scenarios, while baselines exhibit significant performance volatility, MFTune maintains stable and robust speedups exceeding 2.18x. These results confirm that MFTune effectively captures environment-invariant performance patterns through its density-based search space compression and multi-fidelity optimization, allowing for efficient knowledge reuse even under significant shifts in data volume or underlying infrastructure.

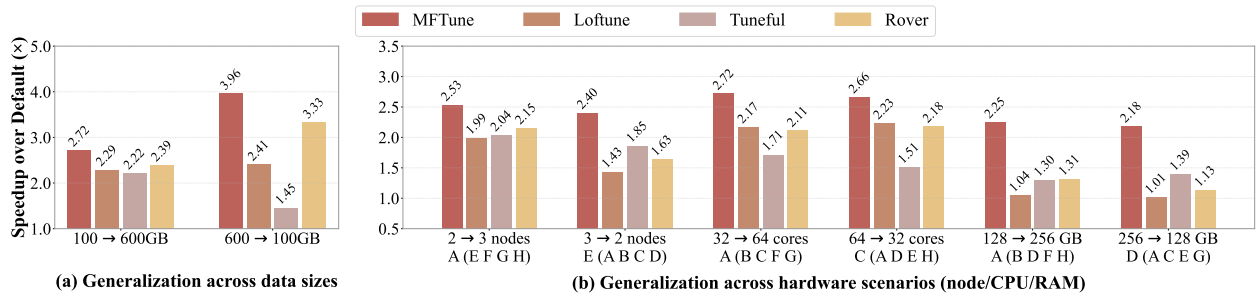


Figure 4: Generalization performance of transfer-learning-based tuning methods across diverse settings. Results represent the speedup of the optimal latency achieved within 48 hours relative to the default Spark configuration.

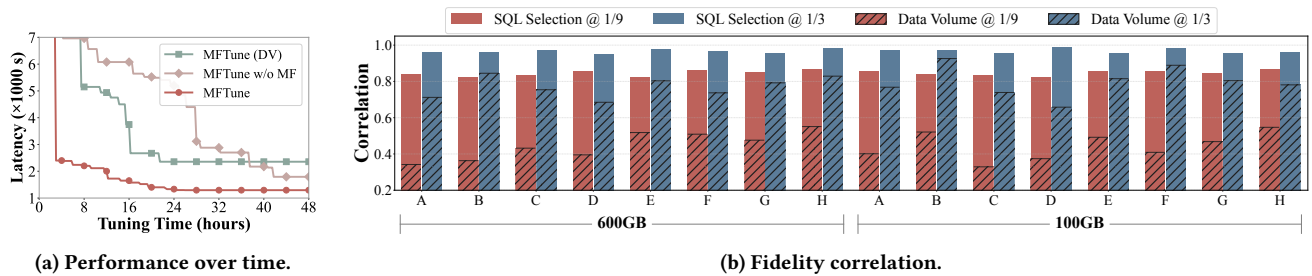


Figure 5: Effectiveness of the multi-fidelity optimization mechanism in TPC-DS benchmark. (a) Ablation study on TPC-DS (600GB) using Hardware A. (b) Fidelity correlation across 16 TPC-DS workloads. Each bar compares the Kendall’s Tau correlation with full fidelity for our SQL Selection method (partitioned via historical observations) versus the Data Volume baseline.

7.4 Detailed Analysis

7.4.1 Analysis of Multi-Fidelity Optimization. In this subsection, we investigate the effectiveness of the MFO mechanism within MFTune using the TPC-DS benchmark. We first conduct an ablation study on Hardware Scenario A with a 600GB data size. Specifically, we compare MFTune against two variants: 1) MFTune w/o MF, which relies exclusively on full-fidelity evaluations like other baselines; and 2) MFTune (DV), which utilizes traditional data volume sampling (i.e., reducing row counts) to create low-fidelity proxies instead of our history-driven SQL selection strategy. Figure 5a illustrates the performance over time for these strategies. Compared to MFTune w/o MF, MFTune achieves significantly faster convergence and finally identifies superior configurations, confirming that the MFO mechanism effectively maximizes the utility of the tuning budget through filtering poor configurations on low-fidelity evaluations. Finally, MFTune achieves a latency reduction of 27.8% over MFTune w/o MF and 45.1% over MFTune (DV). Furthermore, it demonstrates a remarkable acceleration, reaching the final tuning result of MFTune (DV) in just 6.0 hours (an 8.00x acceleration) and matching the final performance of the w/o MF variant in 12.2 hours (a 3.92x acceleration).

Notably, we observe that utilizing data volume as the basis for low-fidelity partitioning even underperforms the baseline that lacks MFO entirely. This occurs because data volume sampling significantly compromises the representation of performance bottlenecks, leading to a diminished correlation with full-fidelity performance. To empirically validate this observation, we analyze the fidelity correlation across all 16 TPC-DS workloads in Figure 5b. The results

demonstrate that our proposed SQL selection method maintains a consistently high correlation—typically above 0.8—even at a low sampling rate of 1/9. This ensures that the ranking of configurations in low-fidelity trials remains highly representative of the full-fidelity. In contrast, the correlation for the data volume (DV) baseline is significantly lower and more volatile, frequently falling below 0.4, which explains why the optimizer is repeatedly misled by inaccurate performance signals in the MFTune (DV) variant.

7.4.2 Analysis of Space Compression. In this section, we evaluate the effectiveness of the search space compression (SC) mechanism in MFTune and analyze the sensitivity of hyperparameter α .

We first compare MFTune’s space compression with the following baselines: 1) *w/o SC*, the original, uncompressed search space. 2) *Box* [38], which suggests a minimal search space containing the best-observed configurations of all the previous tasks. 3) *Decrease*, adopted in Tuneful [8], which removes 40% unimportant knobs every 10 iterations based on the importance ranking generated from the previous observations. 4) *Project*, adopted in LlamaTune [18] and TopTune [54], which projects the original space to a synthetic low-dimensional one and uses bucketization to narrow the value range. 5) *Vote*, adopted in OpAdvisor [65], which extracts boundary values of discrete historical configurations and votes to generate the target space. Specifically, we replace the SC component in MFTune with the aforementioned baseline strategies and conduct end-to-end comparisons on the TPC-H 600GB workload.

Figure 6a illustrates the performance over time for these strategies. MFTune consistently achieves the lowest latency throughout

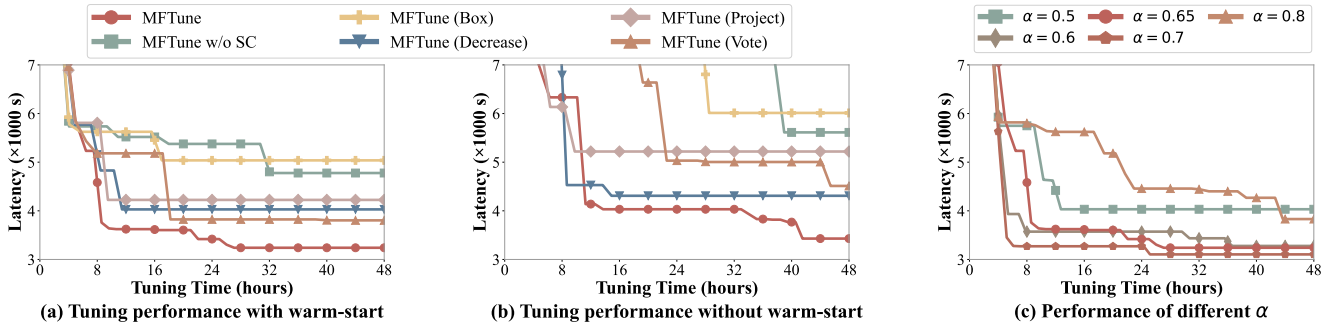


Figure 6: Analysis of the search space compression (SC) mechanism. (a) and (b) present the ablation study of different SC strategies under warm-start and cold-start settings, respectively. (c) Sensitivity analysis of the cumulative density threshold α .

the tuning process, yielding a final latency reduction ranging from 14.8% to 35.7% compared to other SC variants. We observe that although Decrease aims to generate an importance ranking specific to the target task, the initial target observations are often insufficient to accurately rank the knobs, leading to suboptimal pruning. The limitations of existing strategies are evident: Decrease suffers from inaccurate knob ranking due to initial data scarcity; Box often leads to over-pruning by ignoring task-specific differences; and Project lacks the granularity to exclude low-potential subspaces despite reducing dimensionality. While Vote is the most comparable to our approach, its reliance on discrete boundaries makes it highly sensitive to outliers. In contrast, MFTune employs Kernel Density Estimation (KDE) to smooth out noise and pinpoint robust, high-potential regions. To isolate the intrinsic effectiveness of the SC mechanism, we conducted a stress test by disabling the warm-start feature. The rationale is that warm-start can mitigate the impact of a suboptimal search space by directly deploying high-quality historical configurations at the outset. As shown in Figure 6b, the performance gap between MFTune and the other variants widens significantly. In this scenario, MFTune outperforms the other strategies by a larger margin of 20.4% to 43.0%. This demonstrates the robustness of our density-based SC strategy.

Finally, Figure 6c presents the sensitivity analysis of the cumulative density threshold α . We observe that a threshold that is too low (e.g., $\alpha=0.5$) leads to overly aggressive pruning that may exclude the global optimum and cause premature stagnation. Conversely, a threshold that is too high (e.g., $\alpha=0.8$) fails to sufficiently reduce the search dimensionality, resulting in slower convergence similar to the w/o SC baseline. We find that MFTune is highly robust to this hyperparameter within a moderate range, as thresholds of 0.6, 0.65, and 0.7 all yield comparable and stable convergence performance. Consequently, we select $\alpha=0.65$ as the default value.

7.4.3 Ablation Study of Warm Start. In this subsection, we evaluate the individual contributions of the two-phase warm-start strategy. As shown in Table 3, the integrated two-phase approach consistently outperforms both single-phase variants. While Phase 1 (P1) provides a high-quality starting point, Phase 2 (P2) acts as the primary performance driver by synergizing with the MFO mechanism to efficiently filter and exploit a large volume of historical candidates during low-fidelity evaluations. We conclude that this two-phase strategy achieves the most comprehensive utilization of

Table 3: Ablation study of warm-start phases on TPC-H (600GB). P1 and P2 denote Phase 1 warm start and Phase 2 warm start, respectively. All metrics represent the relative gains achieved by MFTune compared to each specific variant.

P1	P2	Latency Reduction (%)	Tuning Acceleration
×	×	5.50%	2.15×
✓	×	5.13%	1.98×
×	✓	1.25%	1.12×

historical data, delivering a 5.50% latency reduction and a 2.15× tuning acceleration over the cold-start baseline by effectively balancing rapid initialization with sustained, cost-effective exploration.

7.4.4 Analysis of Tuning Overhead. We record the computational overhead of MFTune under the original settings. The overhead is categorized into two parts: task-level and iteration-level costs. For task-level initialization, predicting source task similarity requires approximately 15s. Fidelity partitioning—the process of selecting SQL subsets for each fidelity level—takes 21s for TPC-DS compared to 0.5s for TPC-H, a disparity caused by the significantly larger number of queries in the TPC-DS benchmark. At the iteration level, each recommendation round incurs approximately 0.6s for calculating similarity via Kendall rank correlation, 2s for search space compression, and 0.2s for BO to recommend candidate configurations. Collectively, these overheads are negligible when compared to the thousands of minutes required to evaluate a configuration or the total tuning duration spanning dozens of hours.

8 CONCLUSION

In this paper, we propose MFTune, a multi-fidelity framework that overcomes the prohibitive costs and high dimensionality of Spark SQL tuning through query-based fidelity partitioning and density-based search space compression. By integrating a two-phase warm start and adapted transfer learning, MFTune achieves a superior balance between historical knowledge reuse and efficient exploration. Experimental results on TPC-H and TPC-DS benchmarks confirm that MFTune consistently delivers optimal performance across all evaluated settings, significantly outperforming five state-of-the-art methods with negligible computational overhead.

REFERENCES

- [1] Omid Alipourfard, Hongqiang Harry Liu, Jianshu Chen, Shivaram Venkataraman, Minlan Yu, and Ming Zhang. 2017. {CherryPick}: Adaptively unearthing the best cloud configurations for big data analytics. In *14th USENIX Symposium on Networked Systems Design and Implementation (NSDI 17)*. 469–482.
- [2] Michael Armbrust, Reynold S Xin, Cheng Lian, Yin Huai, Davies Liu, Joseph K Bradley, Xiangrui Meng, Tomer Kaftan, Michael J Franklin, Ali Ghodsi, et al. 2015. Spark sql: Relational data processing in spark. In *Proceedings of the 2015 ACM SIGMOD international conference on management of data*. 1383–1394.
- [3] James S Bergstra, Rémi Bardenet, Yoshua Bengio, and Balázs Kégl. 2011. Algorithms for hyper-parameter optimization. In *Advances in neural information processing systems*. 2546–2554.
- [4] Baoqing Cai, Yu Liu, Ce Zhang, Guangyu Zhang, Ke Zhou, Li Liu, Chunhua Li, Bin Cheng, Jie Yang, and Jiashu Xing. 2022. HUNTER: an online cloud database hybrid tuning system for personalized requirements. In *Proceedings of the 2022 International Conference on Management of Data*. 646–659.
- [5] Chao Chen, Jinhan Xin, and Zhibin Yu. 2024. TIE: Fast experiment-driven ml-based configuration tuning for in-memory data analytics. *IEEE Trans. Comput.* 73, 5 (2024), 1233–1247.
- [6] Yuxing Chen, Jiaheng Lu, Chen Chen, Mohammad Hoque, and Sasu Tarkoma. 2019. Cost-effective resource provisioning for spark workloads. In *Proceedings of the 28th ACM International Conference on Information and Knowledge Management*. 2477–2480.
- [7] Stefan Falkner, Aaron Klein, and Frank Hutter. 2018. BOHB: Robust and efficient hyperparameter optimization at scale. In *International conference on machine learning*. PMLR, 1437–1446.
- [8] Ayat Fekry, Lucian Carata, Thomas Pasquier, Andrew Rice, and Andy Hopper. 2020. To tune or not to tune? in search of optimal configurations for data analytics. In *Proceedings of the 26th ACM SIGKDD International Conference on Knowledge Discovery & Data Mining*. 2494–2504.
- [9] Anastasios Gounaris, Georgia Koufka, Ruben Tous, Carlos Tripiñana Montes, and Jordi Torres. 2017. Dynamic configuration of partitioning in spark applications. *IEEE Transactions on Parallel and Distributed Systems* 28, 7 (2017), 1891–1904.
- [10] Yi-Qi Hu, Yang Yu, Wei-Wei Tu, Qiang Yang, Yuqiang Chen, and Wenyuan Dai. 2019. Multi-fidelity automatic hyper-parameter tuning via transfer series expansion. In *Proceedings of the AAAI Conference on Artificial Intelligence*, Vol. 33. 3846–3853.
- [11] Shiyue Huang, Yanzhao Qin, Xinyi Zhang, Yaofeng Tu, Zhongliang Li, and Bin Cui. 2023. Survey on performance optimization for database systems. *Science China Information Sciences* 66, 2 (2023), 121102.
- [12] Frank Hutter, Holger H Hoos, and Kevin Leyton-Brown. 2011. Sequential model-based optimization for general algorithm configuration. In *International Conference on Learning and Intelligent Optimization*. Springer, 507–523.
- [13] Chip Huyen. 2022. *Designing machine learning systems*. " O'Reilly Media, Inc".
- [14] Kevin Jamieson and Ameet Talwalkar. 2016. Non-stochastic best arm identification and hyperparameter optimization. In *Artificial intelligence and statistics*. PMLR, 240–248.
- [15] Huaijun Jiang, Yu Shen, Yang Li, Beicheng Xu, Sixian Du, Wentao Zhang, Ce Zhang, and Bin Cui. 2024. Openbox: A Python toolkit for generalized black-box optimization. *Journal of Machine Learning Research* 25, 120 (2024), 1–11.
- [16] Jiantong Jiang, Zeyi Wen, Atif Mansoor, and Ajmal Mian. 2024. Efficient hyperparameter optimization with adaptive fidelity identification. In *Proceedings of the IEEE/CVF Conference on Computer Vision and Pattern Recognition*. 26181–26190.
- [17] Donald R Jones, Matthias Schonlau, and William J Welch. 1998. Efficient global optimization of expensive black-box functions. *Journal of Global optimization* 13, 4 (1998), 455–492.
- [18] Konstantinos Kanellis, Cong Ding, Brian Kroth, Andreas Müller, Carlo Curino, and Shivaram Venkataraman. 2022. LlamaTune: sample-efficient DBMS configuration tuning. *Proceedings of the VLDB Endowment* 15, 11 (2022), 2953–2965.
- [19] Ralph Kimball and Margy Ross. 2013. *The data warehouse toolkit: The definitive guide to dimensional modeling*. John Wiley & Sons.
- [20] Aaron Klein, Stefan Falkner, Simon Bartels, Philipp Hennig, and Frank Hutter. 2017. Fast bayesian optimization of machine learning hyperparameters on large datasets. In *Artificial intelligence and statistics*. PMLR, 528–536.
- [21] Aaron Klein, Stefan Falkner, Jost Tobias Springenberg, and Frank Hutter. 2017. Learning curve prediction with Bayesian neural networks. In *International conference on learning representations*.
- [22] Aaron Klein, Louis C Tiao, Thibaut Lienart, Cedric Archambeau, and Matthias Seeger. 2020. Model-based asynchronous hyperparameter and neural architecture search. *arXiv preprint arXiv:2003.10865* (2020).
- [23] Jiale Lao, Yibo Wang, Yufei Li, Jianping Wang, Yunjia Zhang, Zhiyuan Cheng, Wanghu Chen, Mingjie Tang, and Jianguo Wang. 2025. GPTuner: An LLM-Based Database Tuning System. *ACM SIGMOD Record* 54, 1 (2025), 101–110.
- [24] Ben Letham, Roberto Calandra, Akshara Rai, and Eytan Bakshy. 2020. Re-examining linear embeddings for high-dimensional Bayesian optimization. *Advances in neural information processing systems* 33 (2020), 1546–1558.
- [25] Guoliang Li, Xuanhe Zhou, Shifu Li, and Bo Gao. 2019. Qtune: A query-aware database tuning system with deep reinforcement learning. *Proceedings of the VLDB Endowment* 12, 12 (2019), 2118–2130.
- [26] Jiahui Li, Junhao Ye, Yuren Mao, Yunjun Gao, and Lu Chen. 2025. LOFTune: A Low-Overhead and Flexible Approach for Spark SQL Configuration Tuning. *IEEE Transactions on Knowledge and Data Engineering* (2025).
- [27] Lisha Li, Kevin Jamieson, Giulia DeSalvo, Afshin Rostamizadeh, and Ameet Talwalkar. 2018. Hyperband: A novel bandit-based approach to hyperparameter optimization. *Journal of Machine Learning Research* 18, 185 (2018), 1–52.
- [28] Lisha Li, Kevin Jamieson, Afshin Rostamizadeh, Katya Gonina, Moritz Hardt, Benjamin Recht, and Ameet Talwalkar. 2018. Massively parallel hyperparameter tuning. (2018).
- [29] Yang Li, Huaijun Jiang, Yu Shen, Yide Fang, Xiaofeng Yang, Danqing Huang, Xinyi Zhang, Wentao Zhang, Ce Zhang, Peng Chen, et al. 2023. Towards General and Efficient Online Tuning for Spark. *Proceedings of the VLDB Endowment* 16, 12 (2023), 3570–3583.
- [30] Yang Li, Yu Shen, Huaijun Jiang, Wentao Zhang, Jixiang Li, Ji Liu, Ce Zhang, and Bin Cui. 2022. Hyper-tune: towards efficient hyper-parameter tuning at scale. *Proceedings of the VLDB Endowment* 15, 6 (2022), 1256–1265.
- [31] Yang Li, Yu Shen, Jiawei Jiang, Jinyang Gao, Ce Zhang, and Bin Cui. 2021. Mfeshb: Efficient hyperband with multi-fidelity quality measurements. In *Proceedings of the AAAI Conference on Artificial Intelligence*, Vol. 35. 8491–8500.
- [32] Scott M Lundberg and Su-In Lee. 2017. A unified approach to interpreting model predictions. *Advances in neural information processing systems* 30 (2017).
- [33] Michael D McKay, Richard J Beckman, and William J Conover. 2000. A comparison of three methods for selecting values of input variables in the analysis of output from a computer code. *Technometrics* 42, 1 (2000), 55–61.
- [34] Felix Mohr and Jan N van Rijn. 2024. Learning curves for decision making in supervised machine learning: a survey. *Machine Learning* 113, 11 (2024), 8371–8425.
- [35] Amin Nayebi, Alexander Munteanu, and Matthias Poloczek. 2019. A framework for Bayesian optimization in embedded subspaces. In *International Conference on Machine Learning*. PMLR, 4752–4761.
- [36] OpenEuler. 2025. *An Open Source OS for Digital Infrastructure*. <https://www.openeuler.org/>
- [37] Emanuel Parzen. 1962. On estimation of a probability density function and mode. *The annals of mathematical statistics* 33, 3 (1962), 1065–1076.
- [38] Valerio Perrone, Huibin Shen, Matthias W Seeger, Cedric Archambeau, and Rodolphe Jenatton. 2019. Learning search spaces for bayesian optimization: Another view of hyperparameter transfer learning. *Advances in neural information processing systems* 32 (2019).
- [39] David Buchaca Prats, Felipe Albuquerque Portella, Carlos HA Costa, and Josep Lluís Berral. 2020. You only run once: spark auto-tuning from a single run. *IEEE Transactions on Network and Service Management* 17, 4 (2020), 2039–2051.
- [40] David Salinas, Jacek Golebiowski, Aaron Klein, Matthias Seeger, and Cedric Archambeau. 2023. Optimizing hyperparameters with conformal quantile regression. In *International Conference on Machine Learning*. PMLR, 29876–29893.
- [41] Raghav Sethi, Martin Traverso, Dain Sundstrom, David Phillips, Wenlei Xie, Yutian Sun, Nezhir Yegitbasi, Haozhun Jin, Eric Hwang, Nileema Shingte, et al. 2019. Presto: SQL on everything. In *2019 IEEE 35th International Conference on Data Engineering (ICDE)*. IEEE, 1802–1813.
- [42] Yu Shen, Xinyuyang Ren, Yupeng Lu, Huaijun Jiang, Huanyong Xu, Di Peng, Yang Li, Wentao Zhang, and Bin Cui. 2023. Rover: An online Spark SQL tuning service via generalized transfer learning. In *Proceedings of the 29th ACM SIGKDD Conference on Knowledge Discovery and Data Mining*. 4800–4812.
- [43] Yu Shen, Beicheng Xu, Yupeng Lu, Donghui Chen, Huaijun Jiang, Zhipeng Xie, Senbo Fu, Nan Zhang, Yuxin Ren, Ning Jia, et al. 2025. A-Tune-Online: Efficient and QoS-Aware Online Configuration Tuning for Dynamic Workloads. In *2025 IEEE 41st International Conference on Data Engineering (ICDE)*. IEEE, 2161–2173.
- [44] Jasper Snoek, Hugo Larochelle, and Ryan P Adams. 2012. Practical bayesian optimization of machine learning algorithms. In *Advances in neural information processing systems*. 2951–2959.
- [45] SparkConf. 2025. *Configuration - Spark 4.0.1 Documentation*. Stanford University. <https://spark.apache.org/docs/latest/configuration.html>
- [46] Wenwen Sun, Zhicheng Pan, Zirui Hu, Yu Liu, Chengcheng Yang, Rong Zhang, and Xuan Zhou. 2025. Rabbit: Retrieval-Augmented Generation Enables Better Automatic Database Knob Tuning. In *2025 IEEE 41st International Conference on Data Engineering (ICDE)*. IEEE, 3807–3820.
- [47] Ashish Thusoo, Joydeep Sen Sarma, Namit Jain, Zheng Shao, Prasad Chakka, Suresh Anthony, Hao Liu, Pete Wyckoff, and Raghotham Murthy. 2009. Hive: a warehousing solution over a map-reduce framework. *Proceedings of the VLDB Endowment* 2, 2 (2009), 1626–1629.
- [48] Robert Tibshirani. 1996. Regression shrinkage and selection via the lasso. *Journal of the Royal Statistical Society Series B: Statistical Methodology* 58, 1 (1996), 267–288.
- [49] Immanuel Trummer. 2022. DB-BERT: a Database Tuning Tool that "Reads the Manual". In *Proceedings of the 2022 international conference on management of*

- data. 190–203.
- [50] Dana Van Aken, Andrew Pavlo, Geoffrey J Gordon, and Bohan Zhang. 2017. Automatic database management system tuning through large-scale machine learning. In *Proceedings of the 2017 ACM international conference on management of data*. 1009–1024.
- [51] Shivaram Venkataraman, Zongheng Yang, Michael Franklin, Benjamin Recht, and Ion Stoica. 2016. Ernest: Efficient performance prediction for {Large-Scale} advanced analytics. In *13th USENIX symposium on networked systems design and implementation (NSDI 16)*. 363–378.
- [52] Junxiong Wang, Immanuel Trummer, and Debabrota Basu. 2022. UDO: Universal Database Optimization using Reinforcement Learning. In *Proceedings of the VLDB Endowment*, Vol. 14. 3402–3414.
- [53] James Warren and Nathan Marz. 2015. *Big Data: Principles and best practices of scalable realtime data systems*. Simon and Schuster.
- [54] Rukai Wei, Yu Liu, Yufeng Hou, Heng Cui, Yongqiang Zhang, and Ke Zhou. 2025. TopTune: Tailored Optimization for Categorical and Continuous Knobs Towards Accelerated and Improved Database Performance Tuning. In *2025 IEEE 41st International Conference on Data Engineering (ICDE)*. IEEE, 613–626.
- [55] Martin Wistuba and Tejaswini Pedapati. 2020. Learning to rank learning curves. In *International Conference on Machine Learning*. PMLR, 10303–10312.
- [56] Jinhua Xin, Kai Hwang, and Zhibin Yu. 2022. Locat: Low-overhead online configuration auto-tuning of spark sql applications. In *Proceedings of the 2022 International Conference on Management of Data*. 674–684.
- [57] Reynold S Xin, Josh Rosen, Matei Zaharia, Michael J Franklin, Scott Shenker, and Ion Stoica. 2013. Shark: SQL and rich analytics at scale. In *Proceedings of the 2013 ACM SIGMOD International Conference on Management of data*. 13–24.
- [58] Zhibin Yu, Zhendong Bei, and Xuehai Qian. 2018. Datasize-aware high dimensional configurations auto-tuning of in-memory cluster computing. In *Proceedings of the Twenty-Third International Conference on Architectural Support for Programming Languages and Operating Systems*. 564–577.
- [59] Matei Zaharia, Mosharaf Chowdhury, Tathagata Das, Ankur Dave, Justin Ma, Murphy McCauley, Michael J Franklin, Scott Shenker, and Ion Stoica. 2012. Resilient distributed datasets: A {Fault-Tolerant} abstraction for {In-Memory} cluster computing. In *9th USENIX symposium on networked systems design and implementation (NSDI 12)*. 15–28.
- [60] Matei Zaharia, Mosharaf Chowdhury, Michael J Franklin, Scott Shenker, and Ion Stoica. 2010. Spark: Cluster computing with working sets. In *2nd USENIX workshop on hot topics in cloud computing (HotCloud 10)*.
- [61] Ji Zhang, Yu Liu, Ke Zhou, Guoliang Li, Zhili Xiao, Bin Cheng, Jiashu Xing, Yangtao Wang, Tianheng Cheng, Li Liu, et al. 2019. An end-to-end automatic cloud database tuning system using deep reinforcement learning. In *Proceedings of the 2019 international conference on management of data*. 415–432.
- [62] Xinyi Zhang, Zhuo Chang, Yang Li, Hong Wu, Jian Tan, Feifei Li, and Bin Cui. 2022. Facilitating database tuning with hyper-parameter optimization: a comprehensive experimental evaluation. *Proceedings of the VLDB Endowment* 15, 9 (2022), 1808–1821.
- [63] Xinyi Zhang, Hong Wu, Zhuo Chang, Shuwei Jin, Jian Tan, Feifei Li, Tieying Zhang, and Bin Cui. 2021. Restune: Resource oriented tuning boosted by meta-learning for cloud databases. In *Proceedings of the 2021 international conference on management of data*. 2102–2114.
- [64] Xinyi Zhang, Hong Wu, Yang Li, Jian Tan, Feifei Li, and Bin Cui. 2022. Towards dynamic and safe configuration tuning for cloud databases. In *Proceedings of the 2022 International Conference on Management of Data*. 631–645.
- [65] Xinyi Zhang, Hong Wu, Yang Li, Zhengju Tang, Jian Tan, Feifei Li, and Bin Cui. 2023. An efficient transfer learning based configuration adviser for database tuning. *Proceedings of the VLDB Endowment* 17, 3 (2023), 539–552.
- [66] Xinyang Zhao, Xuanhe Zhou, and Guoliang Li. 2023. Automatic database knob tuning: A survey. *IEEE Transactions on Knowledge and Data Engineering* 35, 12 (2023), 12470–12490.
- [67] Yiwen Zhu, Subru Krishnan, Konstantinos Karanasos, Isha Tarte, Conor Power, Abhishek Modi, Manoj Kumar, Deli Zhang, Kartheek Muthyala, Nick Jurgens, et al. 2021. Kea: Tuning an exabyte-scale data infrastructure. In *Proceedings of the 2021 International Conference on Management of Data*. 2667–2680.